51st SME North American Manufacturing Research Conference (NAMRC 51, 2023)

Structured light scanning artifact-based performance study

Leah Jacobs[a], Jake Dvorak[a], Aaron Cornelius[a], Ross Zameroski[a], Tim No[b], and Tony Schmitz[a,b]*

aUniversity of Tenneessee, Knoxville, 1512 Middle Drive, Knoxville, TN 37996, USA
bOak Ridge National Laboratory, Manufacturing Demonstration Facility, 2350 Cherahala Blvd., Knoxville, TN 37932, USA

* Corresponding author. Tel.: +1-865-974-6141. *E-mail address:* tony.schmitz@utk.edu.

Abstract

Structured light scanning is used to create a digital twin of a manufactured part, where features are extracted to determine if the part meets the designer's intent and required tolerances. This paper describes repeatability and reproducibility analyses for a commercially-available structured light scanning system and measurement artifact. The repeatability study used five repeated scans at 15 measurement positions. Repeatability was assessed by randomly selecting one of the five scans at each of the 15 positions and creating a part mesh. This process was performed 50 times and the statistics for the dimension variations were calculated to isolate the scanning effects only. The same sequence was then performed for 10 of the 15 positions and five of the 15 positions to evaluate the repeatability sensitivity to the number of measurement positions. Reproducibility was assessed by selecting 15 positions to create a mesh and repeating the 15-position measurement sequence 10 times using different positions for each mesh construction. The statistics for the dimension variations were then calculated. This incorporated the effects of both scanning and the position and orientation of the part relative to the scanner. This sequence was repeated for 10-position and five-position scans to evaluate the corresponding sensitivity. Finally, the artifact dimensions from structured light scanning were compared to coordinate measuring machine measurements of the same features.

 Keywords: Metrology, structured light scanning, repeatability, reproducibility, uncertainty

1. Introduction

Structured light scanning is used to create a three-dimensional rendering of a physical object. The structured light scanner contains a projector which projects a light pattern onto the test object and one or more cameras which capture the distorted pattern created by the object's surface (two cameras are typical). The images captured by the cameras are analyzed to identify the object's shape. Using the calibrated spatial relationship between the projector and cameras, a point cloud is generated showing the exterior surface of the object by stitching multiple images from different positions around the object. The point cloud is polygonized to generate a mesh. This mesh can then be exported as an STL file for analysis, reverse engineering, stock model definition for computer numerical control (CNC) machining paths [1-3], in-process monitoring [4], and location selection for material repair by additive processes, to name a few examples.

This paper describes repeatability and reproducibility analyses for a commercially-available structured light scanner using a selected artifact. The repeatability study used five back-to-back scans at 15 measurement positions (i.e., all five scans were completed at a position before changing the artifact position). Repeatability of the scanning process was assessed by randomly selecting one of the five scans at each of the 15 positions to create the part mesh. This process was repeated 50 times and the feature dimension were extracted using the scanner software. The mean, range, and standard deviation were calculated from the distributions in the feature dimensions to isolate the scanning effects only. The same sequence was then performed for 10 of the 15 positions and five of the 15 positions (same sets of five scans at each position) to evaluate

the repeatability sensitivity to number of measurement positions.

Reproducibility was assessed by selecting 15 positions to create a mesh and repeating the 15-position measurement sequence 10 times using different positions for each mesh construction. The mean, range, and standard deviation were again calculated from the distributions in the feature dimensions. This incorporated the effects of both scanning and the position and orientation of the part relative to the scanner. This sequence was repeated for 10 positions and five positions to evaluate the corresponding sensitivity.

To conclude the study, the artifact was measured using a touch trigger probe coordinate measuring machine (CMM). The structured light scanning feature dimensions were compared to coordinate measuring machine measurements of the same features to determine the errors.

The paper is organized as follows. Background information is provided on prior accuracy assessment for structured light scanning. The repeatability analysis and results are next presented. The reproducibility study approach and results are then reported. The comparison between the CMM and structured light scanning results are given and conclusions are then provided.

2. Background

Structured light scanning has become a well-established instrument for a range of applications [5-9]. Standards for accuracy, repeatability, reproducibility, and acceptance are in progress. For example, ISO Standard 10360-13, Geometrical product specifications (GPS) – Acceptance and reverification tests for coordinate measuring systems (CMS), reached the publishing stage in 2021 [10]. This ISO standard is considered a progression of VDI/VDE 2634 Parts 2 and 3 [11,12]. Additionally, researchers have published many efforts to better understand accuracy in structured light scanning.

Boehm explored the accuracy of consumer-grade structured light scanners by means of flatness, probing, and sphere spacing measurement errors [13]. Eiriksson et al. completed a performance-based analysis of how common parameters effect accuracy on a custom-built structured light system while following VDI/VDE guidelines [14]. Li et al. used a GOM ATOS scanner and a National Physical Laboratory standard freeform artifact to complete a performance test for structured light in various ambient lighting conditions [15]. Polo et al. performed a study on uncertainty and repeatability in structured light scanning by scanning gauge blocks coated with microfine talc powder [16].

Reflectivity and coating of the scanned object can impact accuracy [17,18]. Palousek et al. reported measurement deviation and repeatability for chalk and titanium-coated spheres [19]. Yue et al. proposed a correction algorithm for systematic errors at discontinuities in surface reflectivity [20].

Mendricky introduced a methodology for evaluating structured light scanning accuracy [21]. He defined several metrics for a calibration etalon with precision spheres and applied the proposed methodology using two different GOM ATOS scanners. This test was based on the VDI/VDE 2634 – Part 3 standard, which provides general recommendations for

accuracy evaluation of optical systems. Results showed that measurement uncertainty was within the manufacturer's reported values. Similarly, Zhao et al. completed a comprehensive study for evaluating uncertainty in profile measurements completed using structured light [22]. Experimental results showed that point cloud stitching and registration were the primary uncertainty contributors. They used a bootstrap method to improve computational efficiency compared to the GUM method [23].

Dickin et al. mapped the distortion of a structured light scanner by attaching the scanner to a robot arm and simultaneously measuring the object with a CMM [24]. Three commercially-available scanners were tested and a correction approach was presented. Their research attempted to quantify scan error throughout the scan volume, which is typically difficult and not reported in literature. They concluded that their methodology "provides an exhaustive assessment of the scanner's performance over a chosen scan volume."

3. Measurement setup

The GOM ATOS Q structured light scanner used in this study collects eight million points per scan with two cameras and an LED-based structured light projector. Measurement areas range from 100 mm × 70 mm to 500 mm × 370 mm. The measuring area applied in this study was 350 mm × 260 mm and the working distance was 490 mm. The distances between points varied from 0.04 mm to 0.15 mm. The professional version of GOM Inspect was used to analyze the measurements.

The artifact used for the study was CNC machined from 50.8 mm × 50.8 mm × 101.6 mm 6061-T6 aluminum stock. The geometry included 10 holes with nominal diameters from 2.9 mm to 15.9 mm and four step heights of {20, 25, 30, and 35} mm as shown in Fig. 1. After machining, the prismatic part was grit blasted to a satin finish.
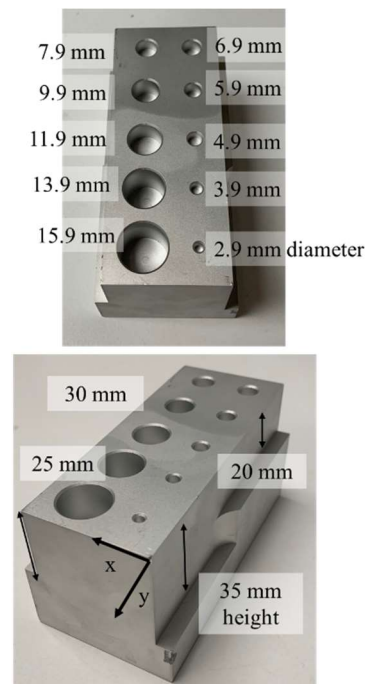

Fig. 1. Artifact with features and nominal dimensions. (Top) 10 holes and (bottom) four step heights and artifact origin.

4. Repeatability

To assess repeatability, five scans were performed back-to-back at 15 positions. The five scans were repeated prior to changing the artifact position. Data sets were prepared by randomly selecting one of the five scans at each position and using the 15 scans to create a mesh. This process was repeated 50 times to obtain 50 separate 15-position measurements. The artifact feature dimensions were then extracted using GOM Inspect software.

For the circle diameters, each hole was fit using a cylinder and the top surface of the artifact was fit using a plane with default software settings. The intersection of the cylinder and plane was used to define a circle and its diameter and center coordinates were recorded for each of the 10 holes; see Fig. 2. The circle center coordinates were described relative to the artifact coordinate system origin shown in Fig. 1. This origin was defined using the intersection of planar fits to the top, front, and right artifact surfaces for the part orientation displayed in the bottom portion of Fig. 1.
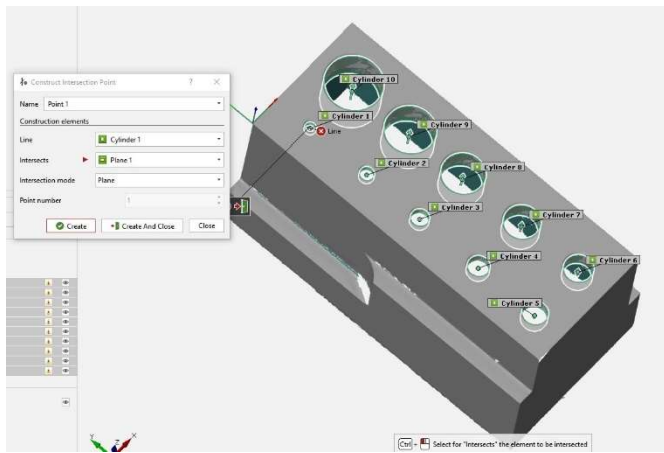
Fig. 2. Circle diameters defined by intersection of cylinders and top surface plane.

For the step heights, planes were also fit to the bottoms of the four steps. The center location of each plane was used to calculate the projected distance between the top and bottom planes in the Z direction, where the Z direction was defined as the surface normal to the best-fit plane for the top surface.
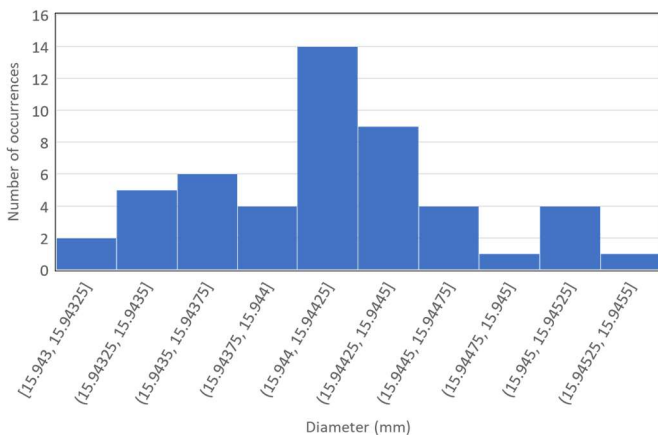

Fig. 3. Example histogram (10 bins, 0.25 μm range for each) for 15.9 mm diameter (largest) circle with 15 scan positions and 50 data sets.

To assess repeatability for the 15-position data sets, feature measurements were completed and the distributions were analyzed. An example histogram is provided in Fig. 3, where an approximately normal distribution is observed for the largest circle (15.9 mm diameter) from the 50 data sets. The mean is 15.944 mm, the range is 2.5 μm, and the standard deviation is 0.5 μm. The scan positions used to obtain the 50 meshes are shown in Fig. 4. These positions did not change for the entire repeatability analysis.
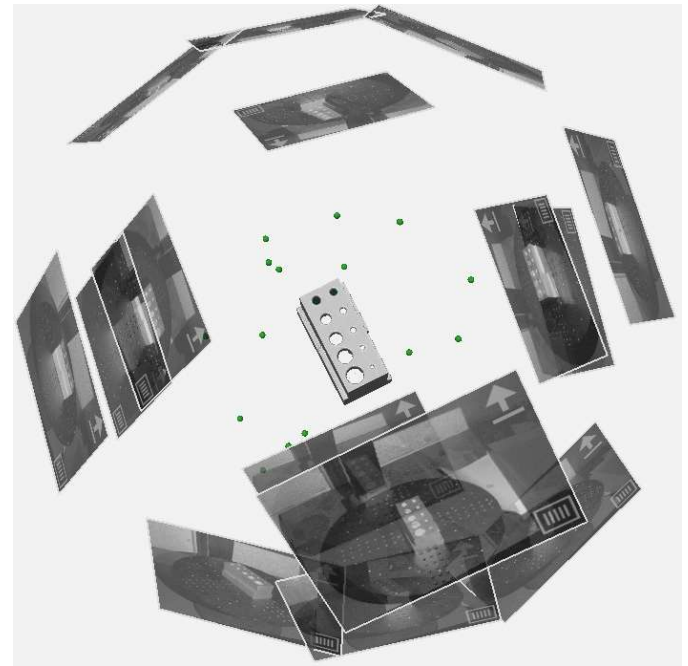

Fig. 4. Scan positions for 15-position repeatability analysis.

The range and standard deviation values from the 50 data sets for all 10 circles are provided in Figs. 5 and 6. It is observed that both values increase dramatically for small circle diameters.
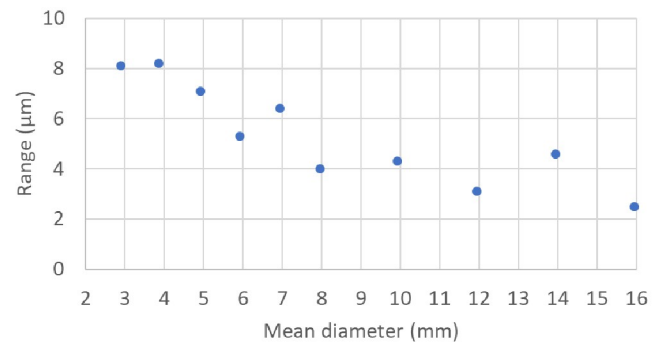

Fig. 5. Circle diameter ranges for 15-position repeatability analysis.

To understand this trend, the number of points used to define the circles (i.e., the number of points at the intersection of the cylinders and top surface plane) was determined. These results are presented in Fig. 7, where each collection of points was fit using a circle to determine the diameter and (x, y) center coordinates. It is seen that number of points on the circle

periphery increases with diameter which, as expected, improves the fit and increases repeatability.
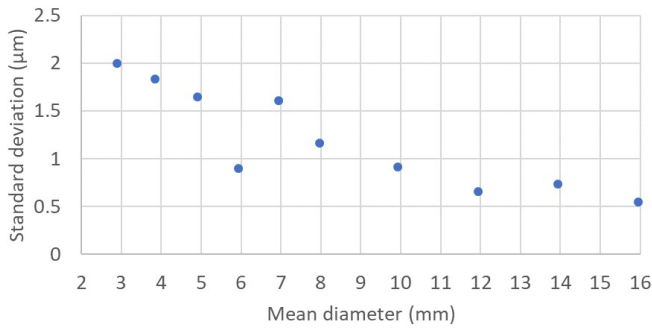

Fig. 6. Circle diameter standard deviations for 15-position repeatability analysis.
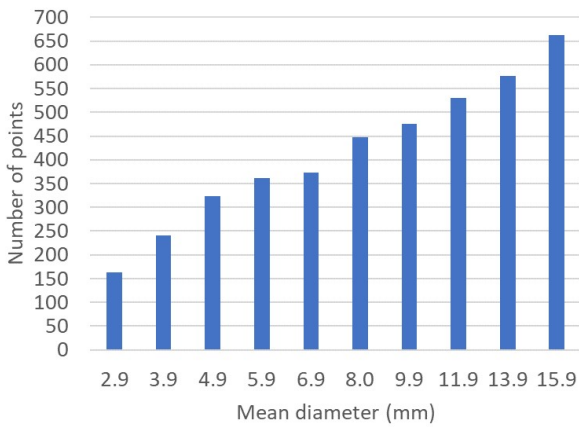

Fig. 7. Number of points on circles for 15-position repeatability analysis.

The center-to-center distances between the 10 circles were calculated for each 15-position data set. The range and standard deviation values are displayed in Figs. 8 and 9, where the two axes in the horizontal plan identify the circle pairs. For example, the range for the distance between the 13.9 mm circle and 2.9 mm circle is 40 µm, as identified by their bar's height at their intersection in the back row, second from right. It is seen that the values decrease for the larger circle pairs and increase when the pair includes smaller circles, particularly the smallest diameter (2.9 mm) circle. This is a direct outcome of the reduced repeatability for the smaller circle fitting.

Fig. 8. Circle center-to-center distance ranges for 15-position repeatability analysis.
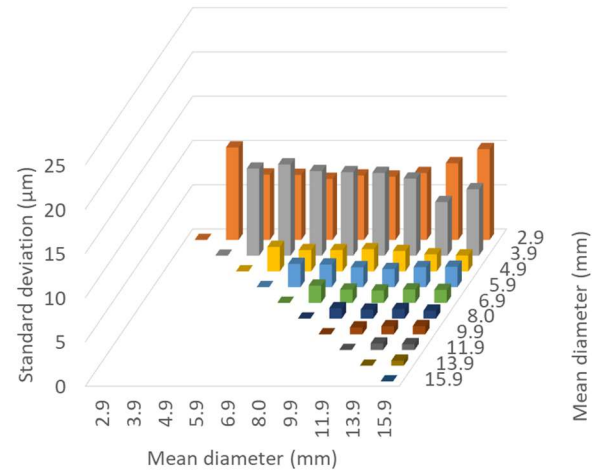
Fig. 9. Circle center-to-center distance standard deviations for 15-position repeatability analysis.
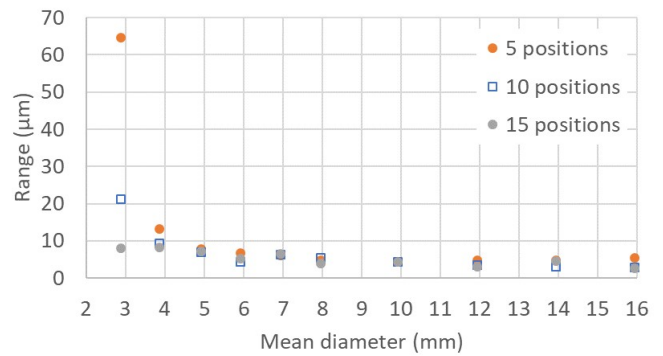

Fig. 10. Comparison of diameter ranges for 10 circles as a function of the number of scanning positions for repeatability analysis.
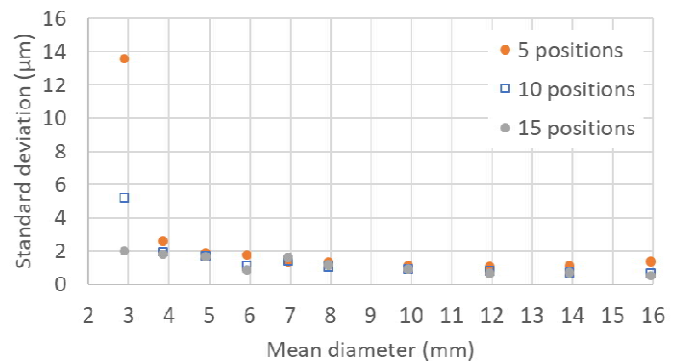

Fig. 11. Comparison of diameter standard deviations for 10 circles as a function of the number of scanning positions for repeatability analysis.
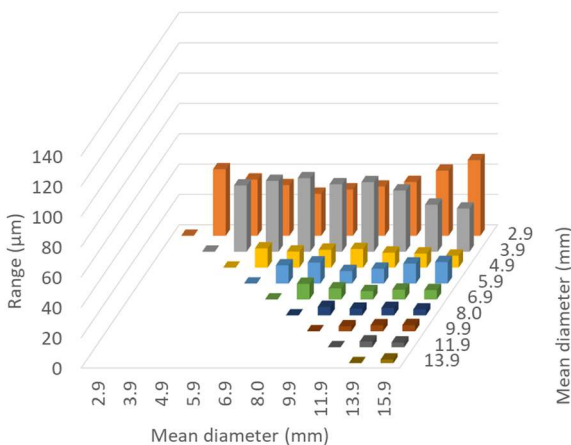
Repeatability was also evaluated when reducing the number of positions used to define the mesh. Tests were performed with 10 and five positions to compare with the 15-position study, where the reduced position meshes were calculated using equally spaced subsets of the positions from the 15-position tests. The mean, range, and standard deviation of the measurements were also calculated for the 10-position and five-position data sets. A comparison of the diameter ranges as a function of mean circle diameter is provided in Fig. 10. The diameter standard deviation comparison is shown in Fig. 11. In both cases, the trend of decreasing range and standard deviation

with increasing circle diameter persists (the number of points on the circles was approximately the same as the 15-position data shown in Fig. 7). In addition, it is seen that reducing the number of scanning positions tends to increase both the range and standard deviation of the circle diameters.
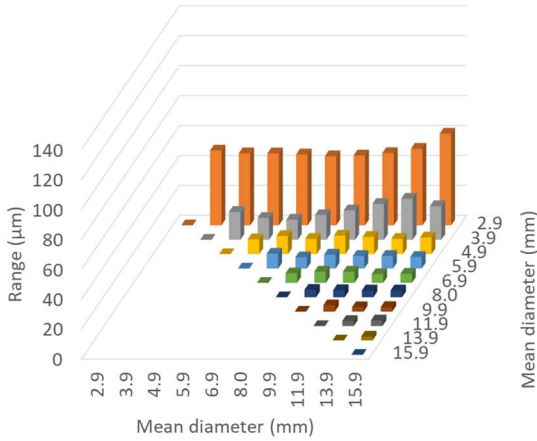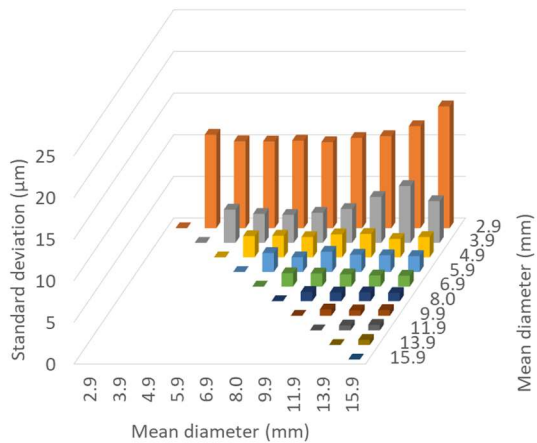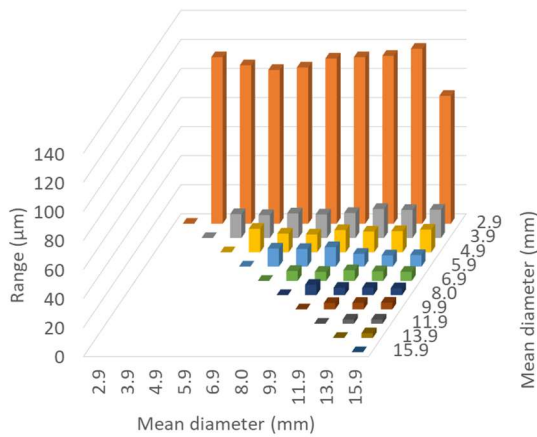
The circle center-to-center distance results are provided in Figs. 12 and 13 for the 10-position data set and Figs. 14 and 15 for the five-position data set. As with the diameter data, the values increase as the number of positions is reduced.

Fig. 12. Circle center-to-center distance ranges for 10-position repeatability analysis.

Fig. 13. Circle center-to-center distance standard deviations for 10-position repeatability analysis.

Fig. 14. Circle center-to-center distance ranges for five-position repeatability analysis.
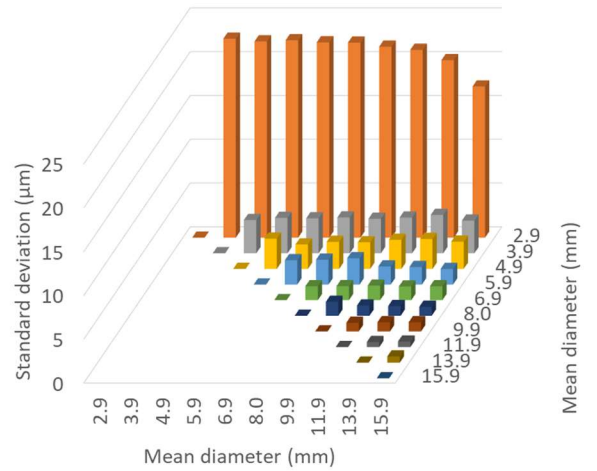

Fig. 15. Circle center-to-center distance standard deviations for five-position repeatability analysis.

The step height results are provided in Figs. 16 and 17. In this case, there is no clear trend in range or standard deviation with step height size. This is because the number of points on the planes used to determine the step heights was not dependent on the step height size. However, an increase in range and standard deviation with a reduced number of scan positions is again observed.
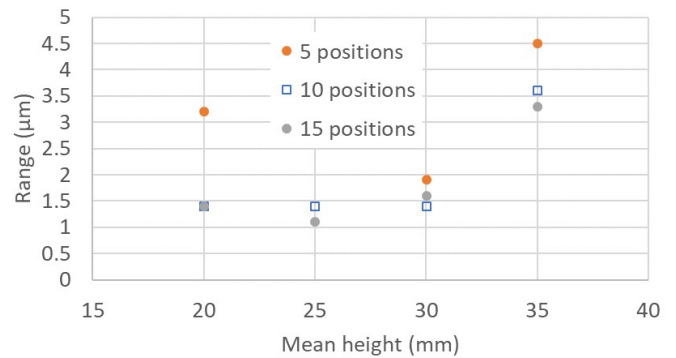

Fig. 16. Comparison of height ranges for four step heights as a function of the number of scanning positions for repeatability analysis.
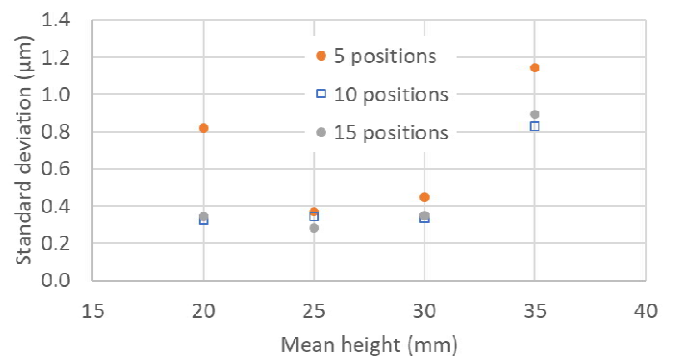

Fig. 17. Comparison of height standard deviations for four step heights as a function of the number of scanning positions for repeatability analysis.

5. Reproducibility

Reproducibility was quantified by selecting 15 positions to create a mesh and repeating the 15-position measurement sequence 10 times using different positions in each case. The measurement positions were varied systematically by placing the artifact on a rotary table located within the structured light scanner's measurement area and changing the rotation angle of the table for each scan. The orientations for 15, 10, and five-position measurements are provided in Table 1. The scan orientations for a 10-position measurement are displayed in Fig. 18 as an example.
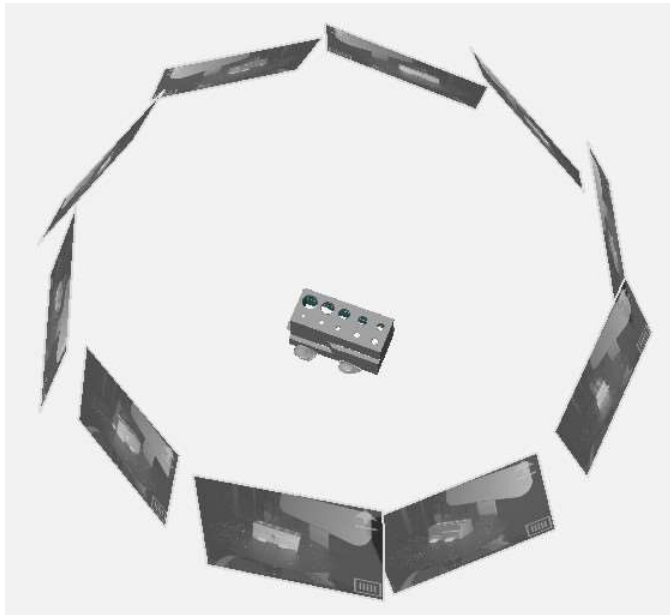

Fig. 18. Scan orientations for a 10-position measurement for reproducibility analysis.

Table 1. Reproducibility scan orientations, where the values are angles (deg) of the rotary table that supported the artifact.

Set	15 positions	10 positions	5 positions
1	0, 24, 50, 70, 96, 120, 145, 170, 190, 215, 240, 265, 290, 315, 335	0, 35, 70, 110, 145, 180, 215, 250, 290, 325	45, 115, 190, 260, 335
2	10, 35, 60, 80, 105, 130, 155, 180, 200, 225, 250, 275, 300, 320, 345	0, 45, 70, 110, 135, 180, 225, 250, 290, 315	10, 80, 155, 225, 300
3	0, 30, 45, 60, 90, 120, 135, 150, 180, 210, 225, 240, 285, 315, 330	20, 45, 90, 135, 155, 200, 225, 270, 315, 335	0, 70, 140, 220, 290
4	10, 40, 55, 70, 100, 130, 145, 160, 190, 220, 235, 250, 295, 325, 340	30, 60, 90, 120, 150, 210, 240, 270, 300, 330	30, 120, 210, 240, 300
5	5, 35, 50, 65, 95, 125, 140, 155, 185, 215, 230, 245, 290, 320, 335	10, 40, 70, 100, 130, 190, 220, 250, 280, 310	50, 120, 190, 250, 330
6	15, 45, 60, 75, 105, 135, 150, 165, 195, 225, 240, 255, 300, 330, 345	20, 50, 80, 110, 140, 200, 230, 260, 290, 320	15, 70, 140, 220, 280
7	20, 50, 65, 80, 110, 140, 155, 170, 200, 230, 245, 260, 305, 335, 350	20, 45, 70, 115, 135, 180, 225, 270, 315, 335	20, 80, 170, 230, 315
8	20, 35, 55, 85, 100, 135, 155, 180, 230, 250, 275, 290, 300, 315, 340	5, 50, 105, 135, 190, 230, 280, 300, 325, 350	25, 70, 145, 245, 320
9	25, 50, 75, 100, 120, 145, 170, 195, 220, 240, 265, 290, 315, 340, 355	25, 55, 90, 125, 160, 240, 275, 300, 320, 355	35, 110, 190, 250, 310
10	5, 20, 50, 65, 95, 110, 140, 185, 200, 230, 245, 275, 290, 320, 335	5, 50, 105, 140, 190, 230, 255, 275, 290, 320	5, 75, 145, 225, 295

The mean, range, and standard deviation were calculated from the dimension distributions. This incorporated the effects of both scanning and the position and orientation of the part relative to the scanner. This sequence was repeated for 10 positions and five positions to evaluate the corresponding sensitivity to number of scan positions; see Table 1. Figure 19 shows a comparison of the diameter ranges as a function of mean circle diameter. The diameter standard deviation comparison is shown in Fig. 20. As with the repeatability study, the range and standard deviation values decrease with increasing circle diameter. Also, reducing the number of scanning positions increase both the range and standard deviation of the circle diameters. Relative to the repeatability results, the ranges and standard deviations are larger for the reproducibility study.
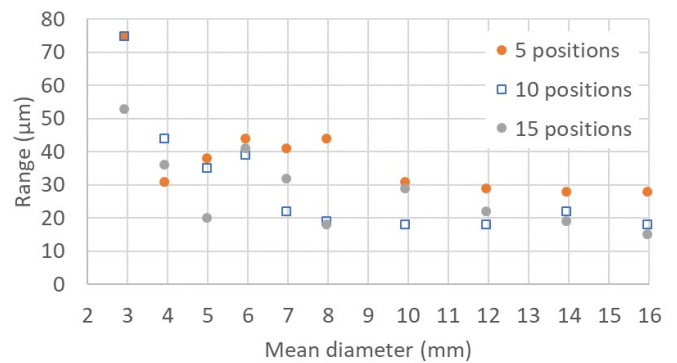

Fig. 19. Comparison of diameter ranges for 10 circles as a function of the number of scanning positions for reproducibility analysis.
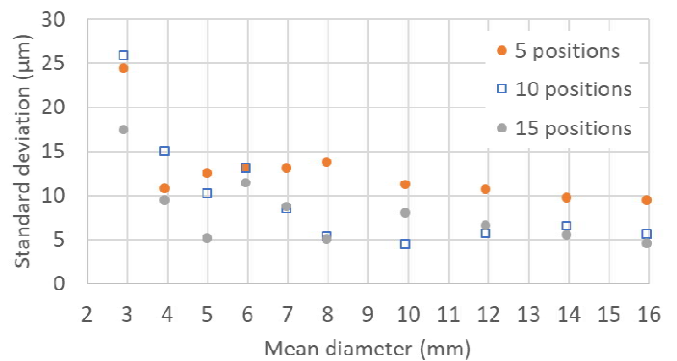

Fig. 20. Comparison of diameter standard deviations for 10 circles as a function of the number of scanning positions for reproducibility analysis.

The circle center-to-center distance results are provided in Figs. 21 and 22 for the 15-position data sets, Figs. 23 and 24 for the 10-position data sets, and Figs. 25 and 26 for the five-position data sets. The reproducibility values are generally larger than the corresponding repeatability values. As with the

repeatability diameter results, the reproducibility decreases as the number of positions is reduced.

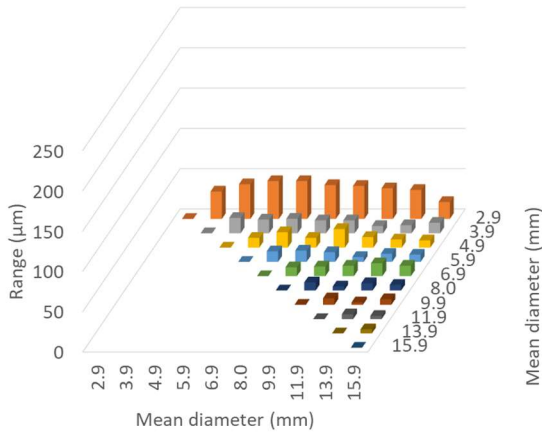and the reproducibility values are significantly larger than the repeatability values.

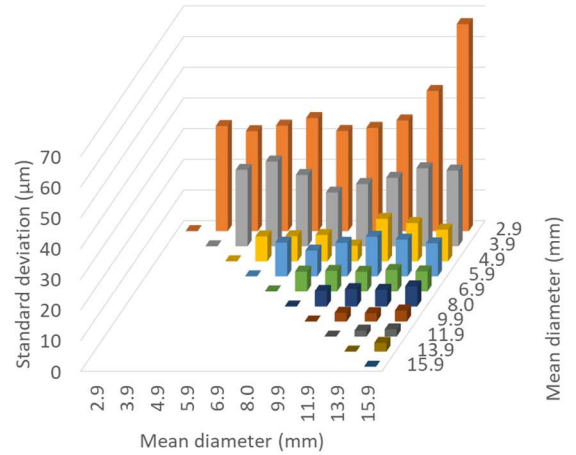Fig. 21. Circle center-to-center distance ranges for 15-position reproducibility analysis.

Fig. 24. Circle center-to-center distance standard deviations for 10-position reproducibility analysis.
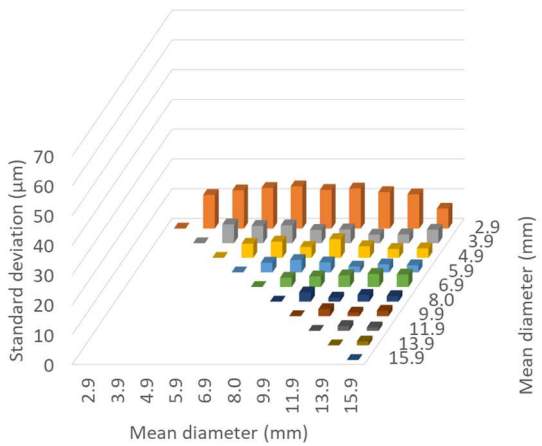

Fig. 22. Circle center-to-center distance standard deviations for 15-position reproducibility analysis.
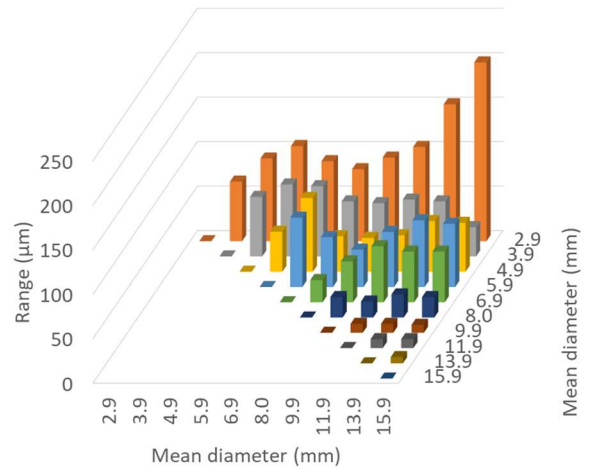

Fig. 25. Circle center-to-center distance ranges for five-position reproducibility analysis.
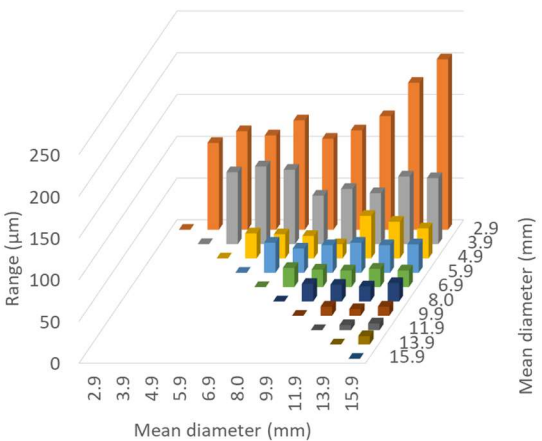

Fig. 23. Circle center-to-center distance ranges for 10-position reproducibility analysis.
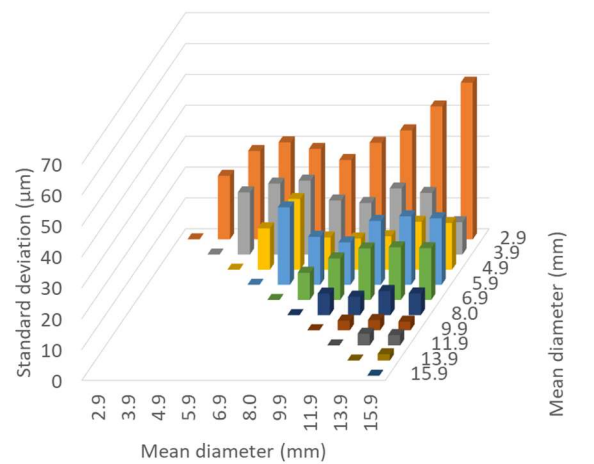

Fig. 26. Circle center-to-center distance standard deviations for five-position reproducibility analysis.

The step height results are displayed in Figs. 27 and 28. There is again no clear trend in range or standard deviation with step height size. An increase in range and standard deviation with a reduced number of scan positions is observed, however,
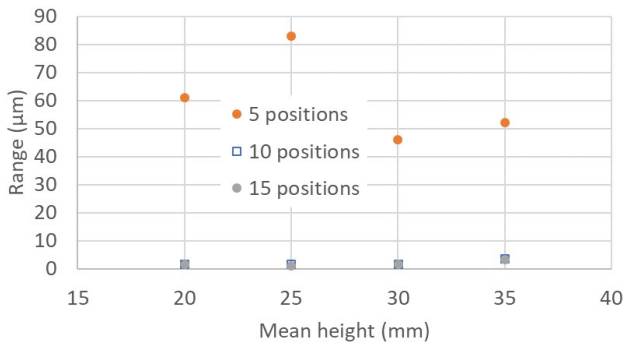
Fig. 27. Comparison of height ranges for four step heights as a function of the number of scanning positions for reproducibility analysis.
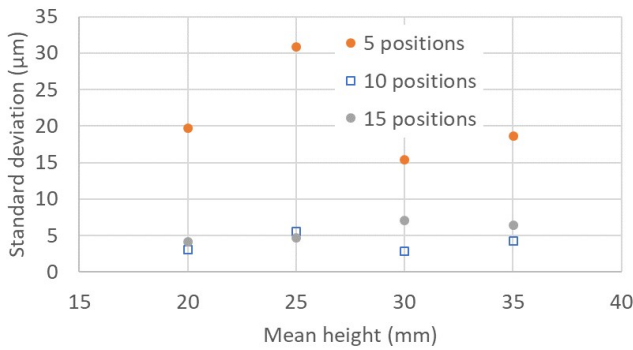

Fig. 28. Comparison of height standard deviations for four step heights as a function of the number of scanning positions for reproducibility analysis.
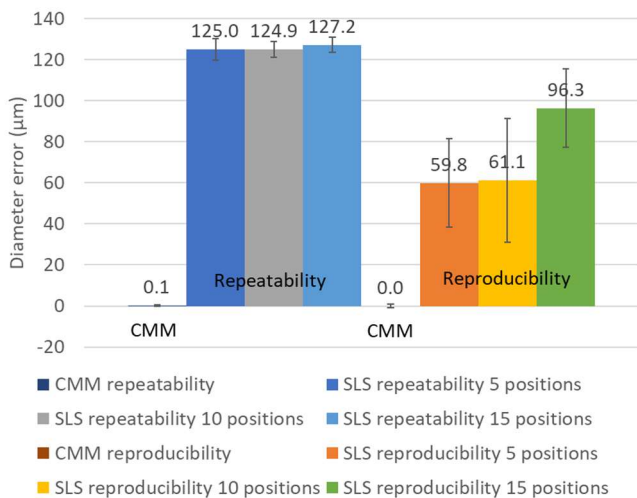

Fig. 29. Error comparison for 3.9 mm diameter hole as a function of the number of scanning positions and measurement system. Note that the CMM repeatability and reproducibility (first two entries on the left) are not visible using the same scale as the SLS results.

6. CMM comparison

A ZEISS DuraMax CMM was used to measure the artifact holes and step heights. The smallest hole could not be measured, however, because its diameter (2.9 mm) was smaller than the probe diameter (3 mm). The repeatability of the CMM measurements was determined by completing 20 measurements using the same artifact location and orientation on the CMM table. Reproducibility was determined by completing 10 measurement sets at random artifact locations and orientations on the CMM table. These measurement results

were compared to the repeatability and reproducibility results for the structured light scanner (SLS). The CMM results provide a comparison between the SLS mean values, as well as their distribution, and the industry standard for dimensional metrology represented by the CMM.

Diameter results are shown in Figs. 29-31. Figure 29 displays a comparison of the error between the CMM and SLS mean values (error = CMM – SLS) for the 3.9 mm diameter (smallest) hole as a function of the number of scanning positions (for the SLS data) and measurement system type. The reference CMM value was the mean value from the reproducibility analysis. The ±one-standard deviation error bars are included. Figure 30 shows the 7.9 mm diameter hole data and Fig. 31 provides the 15.9 mm diameter hole data.

Fig. 30. Error comparison for 7.9 mm diameter hole as a function of the number of scanning positions and measurement system.
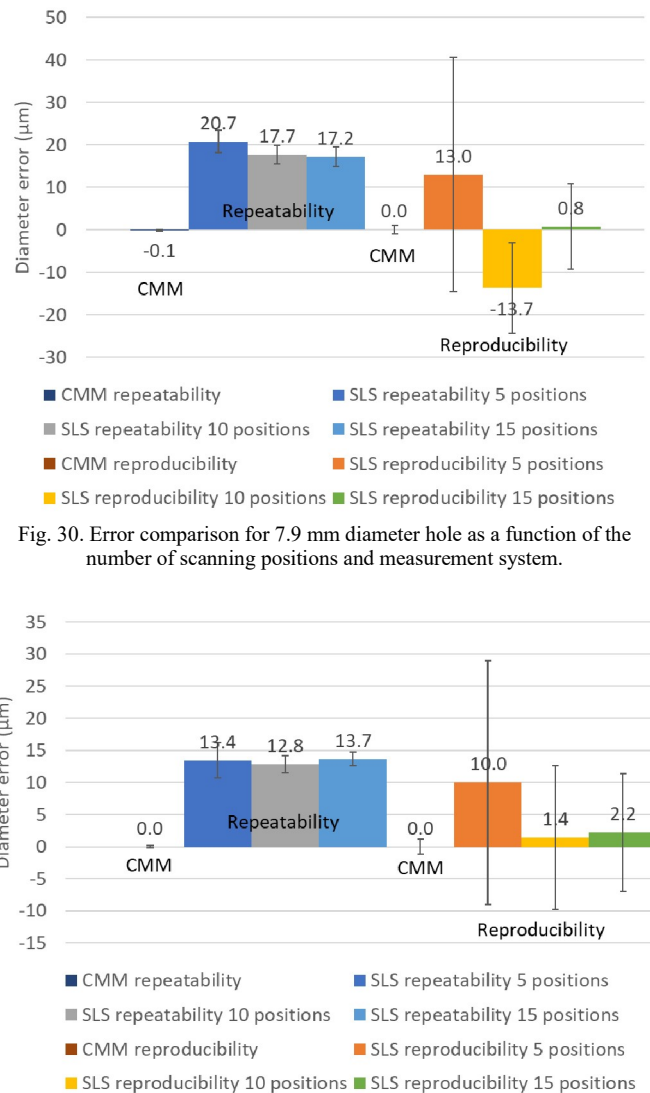

Fig. 31. Error comparison for 15.9 mm diameter hole as a function of the number of scanning positions and measurement system.

A first trend identified from Figs. 29-31 is that the mean diameters from the repeatability study do not agree well with the CMM data and the mean errors do not change appreciably with the number of scan positions. This is expected since all scans were derived from a single data set. However, the errors do decrease with increasing diameter since, as noted

previously, more points are available for fitting the circles with the larger diameters.

A second trend is that the mean diameters from the reproducibility study demonstrate improved agreement with the CMM data. Further, the errors decrease with increasing hole diameter. This suggests that completing multiple measurements with different scan positions for each measurement improve the SLS accuracy.

For the step height values, the SLS step heights are consistently larger than the CMM step heights and the reproducibility results are closer to the CMM results. Since the error bars do not generally overlap, there is a bias between the two instruments. Example results are shown in Fig. 32 for the 25 mm step height difference (CMM – SLS). The results are similar for the other three step heights.
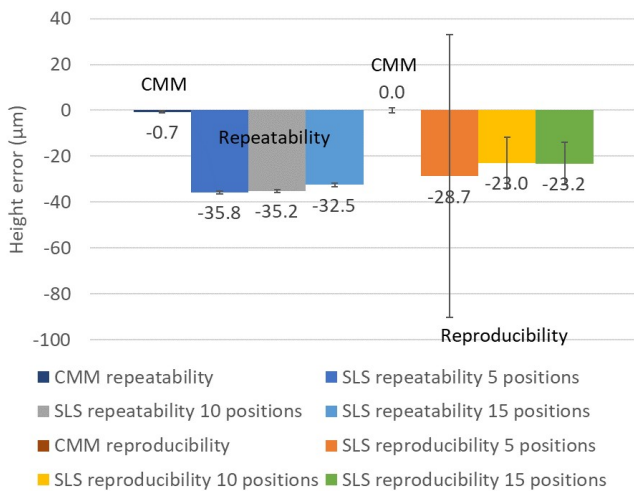

Fig. 32. Comparison of difference from CMM reproducibility for 25 mm step height as a function of the number of scanning positions and measurement system.

7. Conclusions

Structured light scanning (SLS) repeatability and reproducibility studies were completed using artifact measurements. The repeatability study considered variation due to scanning alone. The sensitivity to number of scan positions was also evaluated. It was shown that repeatability increased with the number of scan positions, which was demonstrated by the decreased range and standard deviation found with the larger number of scan positions. It was also shown that the repeatability increased with a larger number of points available on the measurements feature. Specifically, it was seen that larger circles, with more points around the circle periphery, provided increased repeatability.

Reproducibility was assessed by scanning the same part using different positions for each mesh. This analysis included both scanning and artifact position effects on the measurement results. Reproducibility also increased with the number of scan positions and points on the feature. This was confirmed by the decreased range and standard deviation found with the larger number of scan positions and larger circles.

A comparison of the standard deviations from the 10-position repeatability and reproducibility results for all 10 circles is shown in Fig. 33. If viewed individually, this plot

suggests that the best results are obtained for a single part orientation because the standard deviation values are lower. However, from the comparison between the coordinate measuring machine (CMM) and SLS data, it was observed that varying the artifact scan positions between multiple SLS measurements reduced the error between the two measuring systems (with the CMM considered the industry standard).
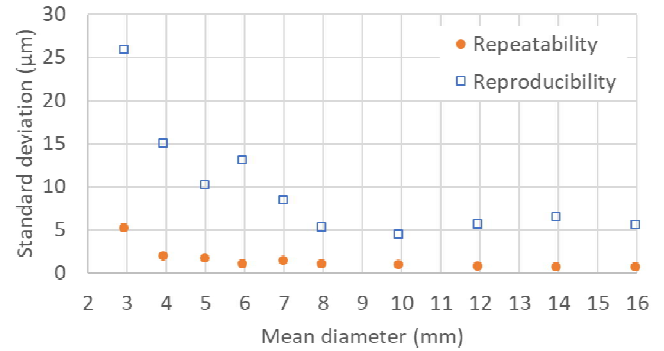

Fig. 33. Comparison of 10-position standard deviations from repeatability and reproducibility analyses for 10 circles.

To summarize the study results, two plots are provided: one for the 10 circles (Fig. 34) and one for the four step heights (Fig. 35). The vertical axis in each plot gives the number of measurement positions and the horizontal axis gives the feature size. The height map shows the reproducibility (one standard deviation) from 10 separate tests for each of the feature size-number of position combinations. The units are micrometers.
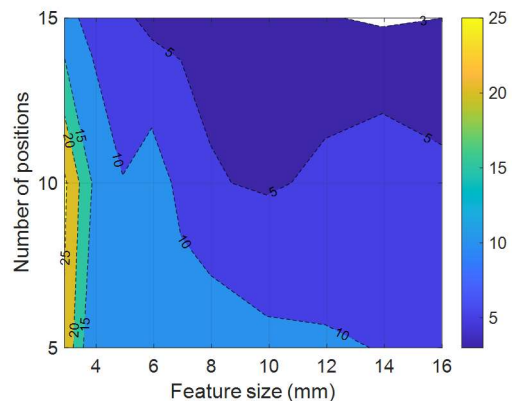

Fig. 34. Circle measurement reproducibility as a function of feature size and number of positions (color bar units are µm).
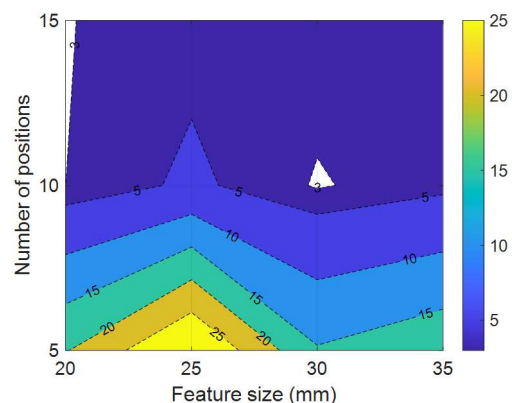

Fig. 35. Step height measurement reproducibility as a function of feature size and number of positions (color bar units are µm).

The outcome is that for the circles, with a dependence of the number of points used to define the feature on its size (see Fig. 7), low standard deviations (5 µm or less) are only available for a large number of measurement positions (10 to 15) and moderate to large circles (6 mm to 16 mm).

For the step heights, on the other hand, there is no strong dependence on the feature size (i.e., the contours are approximately flat). This is because the artifact geometry provided approximately the same surface area for measurements regardless of the step height. Low standard deviations (5 µm or less) are only available for a large number of measurement positions (10 to 15).

Acknowledgements

References

[1] Dvorak, J., Cornelius, A., Corson, G., Zameroski, R., Jacobs, L., Penney, J. and Schmitz, T., 2022, A Machining Digital Twin for Hybrid Manufacturing, Manufacturing Letters, 33: 786-793.

[2] Cornelius, A., Jacobs, L., Lamsey, M., McNeil, L., Hamel, W. and Schmitz, T., 2022, Hybrid Manufacturing of Invar Mold for Carbon Fiber Layup using Structured Light Scanning, Manufacturing Letters, 33: 133-142.

[3] Cornelius, A., Dvorak, J., Jacobs, L., Penney, J., and Schmitz, T., 2021, Combination of Structured Light Scanning and External Fiducials for Coordinate System Transfer in Hybrid Manufacturing, Journal of Manufacturing Processes, 68: 1824-1836.

[4] Wang, R., Wang, Y., Devadiga, S., Perkins, I., Kong, Z.J. and Yue, X., 2021. Structured-light three-dimensional scanning for process monitoring and quality control in precast concrete production. PCI Journal, 66(6).

[5] McPherron, S.P., Gernat, T. and Hublin, J.J., 2009. Structured light scanning for high-resolution documentation of in situ archaeological finds. Journal of Archaeological Science, 36(1), pp.19-24.

[6] Dastoorian, R., Elhabashy, A.E., Tian, W., Wells, L.J. and Camelio, J.A., 2018, June. Automated surface inspection using 3D point cloud data in manufacturing: A case study. In International manufacturing science and engineering conference (Vol. 51371, p. V003T02A036). American Society of Mechanical Engineers.

[7] Rodríguez-Martín, M., Rodríguez-Gonzálvez, P., Gonzalez-Aguilera, D. and Fernandez-Hernandez, J., 2017. Feasibility study of a structured light system applied to welding inspection based on articulated coordinate measure machine data. IEEE Sensors Journal, 17(13), pp.4217-4224.

[8] Pezzuolo, A., Guarino, M., Sartori, L. and Marinello, F., 2018. A feasibility study on the use of a structured light depth-camera for three-dimensional body measurements of dairy cows in free-stall barns. Sensors, 18(2), p.673.

[9] Xu, J., Xi, N., Zhang, C., Shi, Q. and Gregory, J., 2011. Real-time 3D shape inspection system of automotive parts based on structured light pattern. Optics & Laser Technology, 43(1), pp.1-8.

[10] ISO 10360-13:2021 - Geometrical product specifications (GPS) — Acceptance and reverification tests for coordinate measuring systems (CMS) — Part 13: Optical 3D CMS

[11] VDI/VDE Standard citation VDI/VDE 2634 BLATT 2. Optical 3-D measuring systems - Optical systems based on area scanning. 2012.

[12] VDI/VDE 2634 BLATT 3. Optical 3D-measuring systems - Multiple view systems based on area scanning. 2008.

[13] Boehm, J., 2014. Accuracy investigation for structured-light based consumer 3D sensors. Photogrammetrie-Fernerkundung-Geoinformation, 2014(2), pp.117-127.

[14] Eiríksson, E.R., Wilm, J., Pedersen, D.B. and Aanæs, H., 2016. Precision and accuracy parameters in structured light 3-D scanning. International Archives of the Photogrammetry, Remote Sensing and Spatial Information Sciences, 5, p.W8.

[15] Li, F., Stoddart, D. and Zwierzak, I., 2017. A performance test for a fringe projection scanner in various ambient light conditions. Procedia CIRP, 62, pp.400-404.

[16] Polo, M.E., Cuartero, A. and Felicísimo, Á.M., 2019. Study of uncertainty and repeatability in structured-light 3D scanners. arXiv preprint arXiv:1910.13199.

[17] Yang, Y., Chen, S., Wang, L., He, J., Wang, S.M., Sun, L. and Shao, C., 2019, June. Influence of coating spray on surface measurement using 3D optical scanning systems. In International Manufacturing Science and Engineering Conference (Vol. 58745, p. V001T02A009). American Society of Mechanical Engineers.

[18] Li, B., Xu, Z., Gao, F., Cao, Y. and Dong, Q., 2022. 3D Reconstruction of High Reflective Welding Surface Based on Binocular Structured Light Stereo Vision. Machines, 10(2), p.159.

[19] Palousek, D., Omasta, M., Koutny, D., Bednar, J., Koutecky, T. and Dokoupil, F., 2015. Effect of matte coating on 3D optical measurement accuracy. Optical Materials, 40, pp.1-9.

[20] Yue, H., Dantanarayana, H.G., Wu, Y. and Huntley, J.M., 2019. Reduction of systematic errors in structured light metrology at discontinuities in surface reflectivity. Optics and Lasers in Engineering, 112, pp.68-76.

[21] Mendricky, R., 2016. Determination of measurement accuracy of optical 3D scanners. MM Science Journal, 2016(6), pp.1565-1572.

[22] Zhao, Y., Cheng, Y., Xu, Q., Luo, Z., Wang, X. and Li, H., 2022. Uncertainty modeling and evaluation of profile measurement by structured light scanner. Measurement Science and Technology, 33(9), p.095018.

[23] ISO/IEC Guide 98-3:2008. Uncertainty of measurement — Part 3: Guide to the expression of uncertainty in measurement (GUM:1995)

[24] Dickin, F., Pollard, S. and Adams, G., 2021. Mapping and correcting the distortion of 3D structured light scanners. Precision Engineering, 72, pp.543-555.